PROCEEDINGS OF THE SOCIETY FOR EXPERIMENTAL BIOLOGY AND MEDICINE 169, 506–518 (1982)

Histologic Monitoring of Murine Mammary Tumor Lysis Induced by an Autologous Serum Factor[1] (41382)

MARTIN ROY,* FRANK FRIEDMAN,*,† SAM J. PILIERO,* MYRON JACOBS,‡ ROBERT A. BONOMO,* AND HOWARD S. GROB†

*Department of Histology and Cell Biology, New York University College of Dentistry, and Graduate School of Arts and Science, New York, New York 10010; †Biology Department, Adelphi University, Garden City, New York 11530; ‡Department of Pathobiology and Oral Pathology, New York University College of Dentistry, and Graduate School of Arts and Science, New York, New York 10010

Abstract. An autotumorolytic factor (SFIII), derived from a serum fraction of mammary tumor-bearing mice, has been demonstrated to be active when injected into the donor mouse. Gross and histologic assessment of tumors was made at 3, 12, 24, 48, 72, and 96 hr postinjection of SFIII. Concomitantly, lymph node, spleen, liver, kidney, thymus, and lung tissues were examined in these treated tumor animals and compared to non-tumor-bearing animals and a single animal exhibiting spontaneous tumor breakdown. Tumor destruction began at 3 hr postinjection with interlobular connective tissue breakdown accompanied by hemorrhage. Infiltration of connective tissue, where still present, by lymphocytes, plasma cells, and macrophages progressively increased with time. Lysis of tumor tissue subsequently spread to intralobular epithelium resulting in large cavitations containing fragmented tissue and debris, characterized by coagulative and liquefactive necrosis and caseation. Lymphoid tissues showed no significant immune reactivity. This pattern of induced tumorolysis appeared to have been duplicated in spontaneous tumor breakdown. Liver, lung, kidney, and the normal mammary tissue were apparently unaffected by the tumorolytic factor.

The histology of murine mammary adenocarcinoma was first reported by Apolant in 1906. In the ensuing decades, the experimental neoplastic model has become an important tool for extensive and diverse investigations encompassing the disciplines of genetics, endocrinology, virology and, more recently, immunology (1–4). Concomitant with these studies, there has emerged a histopathological description of this murine mammary neoplasm in a variety of strains (5–8). The histological appearance of this animal's mammary tumor most closely resembles that of type-A adenocarcinoma in the Dunn classification (5). In all terminal animals, some necrosis can be detected, localized either within a single region of a lobule or diffusely disseminated as foci throughout the entire tumor mass.

In a previous communication (9), it was reported that an autotumorolytic factor could be extracted from the serum of a tumor-bearing host. When this refined factor was subcutaneously injected into the tumor-bearing donor animal, a significant reduction in the mass of the palpable tumor occurred within 48–72 hr postinjection. This reduction was manifested as a gross disorganization and breakdown of the neoplasm.

The purpose of the current study was to determine the cytological and histological nature of tumor destruction as well as the sequential phasing of tumor lysis.

Materials and Methods. The animal system used in these studies was the C3H(T/F) mouse, derived from the original Bittner C3H strain (10, 11), which has been maintained and inbred in our laboratories for over 20 years. Every female develops mammary adenocarcinoma, usually be-

[1] This research was supported by funds from the Arde Bulova Memorial Fund, Inc.; the Ethel Brown and Percival E. Foerderer Foundation; the Laidlaw Foundation; and the Histology Research Fund of the NYU College of Dentistry.

0037-9727/82/040506-13$01.00/0
Copyright © 1982 by the Society for Experimental Biology and Medicine.
All rights reserved.

tween 5 and 12 months of age, and succumbs to the tumor in an average of 56 days from the time the tumor becomes palpable (50 mm^3).

C3H(T/F) mice, 6–9 months of age and bearing 2-week-old tumors, based on the time of initial palpation, were used in the present experiments. Animals were individually bled by orbital sinus puncture, and the autotumorolytic factor (SFIII) was extracted from each serum sample according to a modification of the original extraction technique (9). This procedure was modified as follows: 0.2 ml of serum was diluted with 1.3 ml of a sodium–potassium phosphate buffer, prepared by titrating 0.05 *M* Na_2HPO_4 solution with 0.05 *M* KH_2PO_4 solution to pH 7.5. The diluted serum was then centrifuged at 6500*g* for 4 min at 1–4°. The supernatant material was then processed as indicated in Fig. 1. The final sediment (SFIII) was resuspended in 0.5 ml of the sodium–potassium phosphate buffer for injection.

Each animal was injected, subcutaneously, with its own factor extract (SFIII), no more than 1 hr after the preparation of the active fraction, at a site as far removed from the tumor as possible. In all animals, the entire resuspended sediment (0.5 ml) was injected.

The experimental C3H(T/F) animals were divided into subgroups of three or four mice. Subgroups were sacrificed and autopsied at 3, 12, 24, 48, 72, and 96 hr postinjection. Untreated or buffer-injected tumor-bearing animals were also sacrificed at various times (2–6 weeks) after initial palpation of the tumor. Female mice (3–7 months of age) from a non-tumor-bearing control strain (C3Hf), Caesarean derived from the original C3H tumor strain, and foster nursed on lactating mice of a non-tumor strain, were also autopsied. In addition, one animal from the C3H(T/F) group, exhibiting spontaneous breakdown of a large tumor, died and was similarly examined.

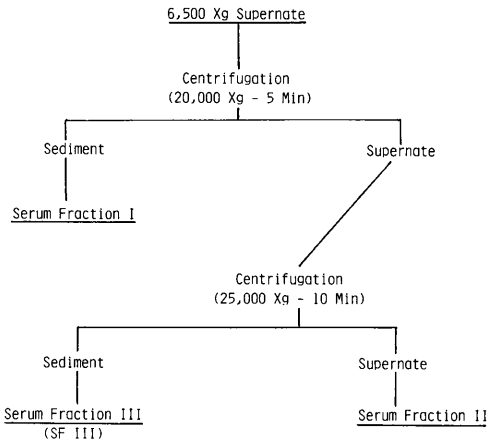

FIG. 1. Procedure for the extraction of the autotumorolytic factor (SFIII).

Histopathologic assessment was made of the tumor and/or mammary tissue in each animal. In addition, the lymphoid organs (nodes, spleen, and thymus) as well as the liver, lungs, and kidneys of all animals were examined microscopically. All tissues and organs were examined grossly prior to: fixation in 10% neutral buffered formalin, embedding in Paraplast, sectioning at 5 μm, and routine staining with Harris–Lillie hematoxylin and eosin (12). Sections were examined at various depths through each processed tumor and organ.

Results. *Normal mammary gland.* The mammary gland of the normal C3Hf mouse (Fig. 2) consists of a branched system of ducts and tubules lying in a stroma of well-vascularized adipose connective tissue, which is continuous with the hypodermis. Lactiferous ducts are lined by stratified columnar epithelium and occasionally eosinophilic debris of likely protein origin is seen in the lumen. The tubules are composed of columnar epithelium. With increasing age, the tubular system becomes well developed, with greater branching, and occupies a larger portion of the total gland relative to the connective tissue. Glandular acini are relatively rare at 3 months and become more evident at 6 months. The glandular epithelium is cuboidal with a relatively small amount of eosinophilic cytoplasm, which shows no secretory activity. The nuclei are small and dark staining with nucleoli which are occasionally visible. Both a distinct lamina propria and myoepithelial basket cells are present.

Tumorous mammary gland. Single or

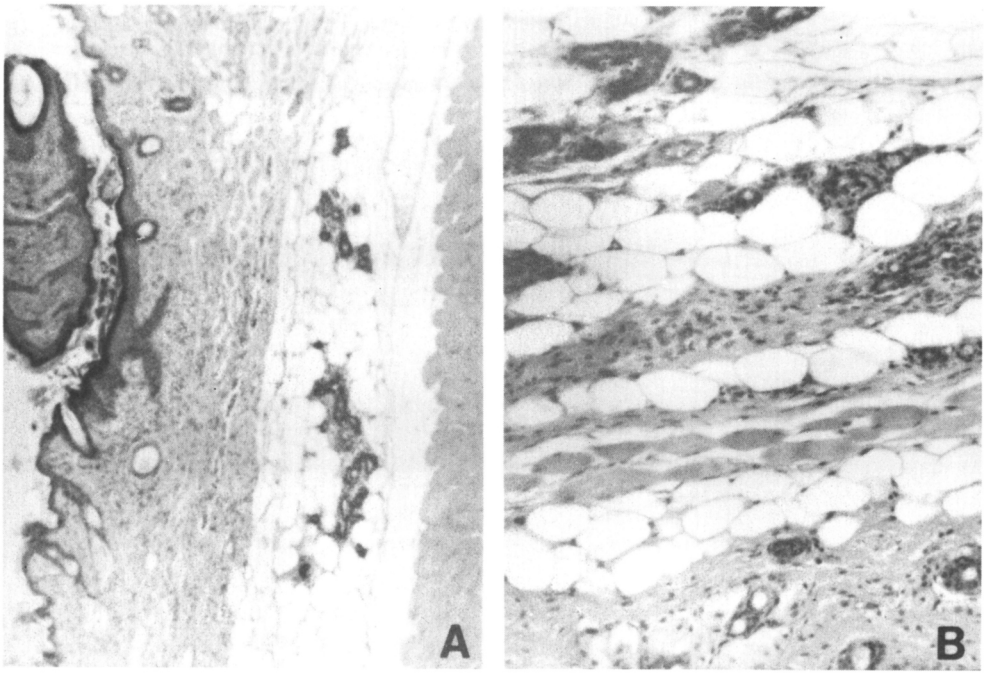

FIG. 2. Mammary gland of a normal C3Hf mouse. (A) At 3–4 months of age (mag. 60×); and (B) at 6–7 months of age (mag. 150×).

multiple masses could be found associated with any of the 10 mammae and, occasionally, on the dorsolateral body surface. Both untreated and buffer-injected mice displayed similar gross and microscopic appearances. Two-week-old tumors had a mean volume of 300 mm^3 and reached 5000–10,000 mm^3 by 5–6 weeks. All tumors remained fixed to the connective tissue. Two-week-old tumors, ovoid or slightly irregular in shape, were smooth or nodular, hard to firm in consistency, and contained no apparent cystic areas. Five- to six-week-old tumors were extremely nodular with alternating gray and white surfaces interspersed with ecchymotic foci. Upon hemisection, 2-week tumors presented white glistening cut surfaces containing a few petechiae, while 5- to 6-week tumors, which invariably exhibited some soft and boggy areas, presented a mottled, hemorrhagic surface, which sometimes contained milky white or cheesy material.

Untreated and buffer-injected mice displayed mammary tumors typical of those described as type A adenocarcinoma (5). The tumor mass (Fig. 3A) consisted predominantly of uniform solid neoplastic acini lined by cuboidal epithelium. Compared to normal mammary epithelium, neoplastic cell nuclei were often pleomorphic and usually stained less intensely, while the cytoplasm was greatly increased in amount and sometimes appeared vacuolated. Hyperchromatic nuclei were also present. Mitotic figures were often seen. Interlobular connective tissue was sparse, but the tumor mass retained marked vascularity. However, the overall architecture of the mammary gland was recognizable. The tumor, nevertheless, was invasive and a sharp line of demarcation between affected and unaffected regions of the mammary gland was frequently absent.

Though very young tumors (<50 mm^3) rarely showed any degenerative changes, tumors that were over 2 weeks old usually displayed some small areas of focal necrosis. Younger tumors (2 weeks old) occasionally showed infiltration of the connective tissue by polymorphonuclear leukocytes (PMNs), monocytes, lymphocytes,

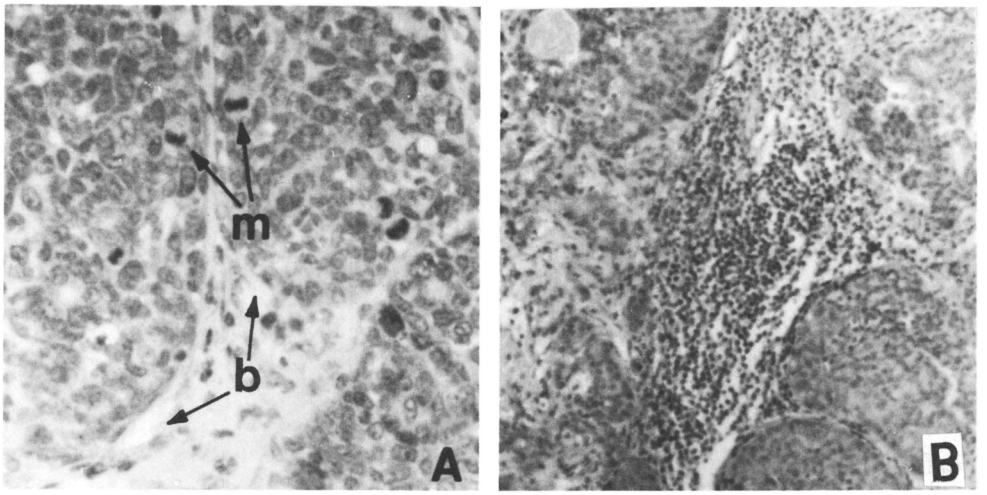

FIG. 3. Mammary tumors of uninjected host C3H(T/F) mice at 2 weeks postinitial palpation of the tumor (<50mm^3). Mitotic figures (m) in the epithelium and blood vessels (b) in the connective tissue are present (A) (mag. 300×). Inflammatory cell infiltration of the connective tissue (B) is occasionally evident at this time (mag. 150×).

and occasional plasma cells (Fig. 3B). In older tumors (3–4 weeks), larger areas of tissue breakdown, manifested by patterns of coagulative, liquefactive, and caseous necrosis, could be seen. Many of the blood vessels present were congested. In terminal stages (5–6 weeks old), large cavitations containing proteinaceous debris were often present in the tumor parenchyma.

Tumorous mammary glands of SFIII-treated mice. Injection of SFIII into animals with 2-week-old tumors resulted in a reproducible set of changes which, for the most part, were constant in any given experimental group, based on the time after the initiation of treatment.

At 3 hr postinjection, neither the volume nor gross appearance of these tumors had changed. Histologically, many regions of the tumor were, as yet, unaffected and mitotic activity was still evident. However, affected regions (usually central lobules) showed localized infiltrations by lymphocytes, PMNs, and occasionally plasma cells in the perivascular areas of the interlobular connective tissue (Figs. 4A, B). Occasionally, ruptured blood vessels and interlobular hemorrhage (Fig. 4A) and signs of intraacinar degeneration and necrosis (e.g., cloudy swelling, ballooning degeneration, and pyknosis) were observed. Several incomplete acini were encountered, which may have resulted from necrotic foci.

Twelve hours after injection with SFIII, no change in volume could be determined. The interior surface exhibited a few distinctive hemorrhagic and necrotic foci. Microscopically, some tumorous lobules or entire lobes were still intact. Degradative changes appeared to be initiated in the connective tissue surrounding the acini and lobules, such changes being heralded by congestion of all blood vessels and by an inflammatory cellular exudate of predominantly mononuclear nature (Fig. 5A). In some areas (Fig. 5B), the connective tissue had broken up and disappeared. Many areas of tumor (Fig. 5C) exhibited pronounced breakdown of tumor cells within the acini, near the inflammatory foci. Lactiferous ducts (Fig. 5D) became filled with proteinaceous fluid, cell debris, isolated tumor cells, and inflammatory cells. Areas of hemorrhage were present in the remaining connective tissue (Figs. 5B, D). Occasionally, a 3-hr postinjection animal exhibited the same degree of tumor breakdown as the 12-hr samples.

The volume of some 24-hr postinjection tumors had decreased by 15–20%. Other

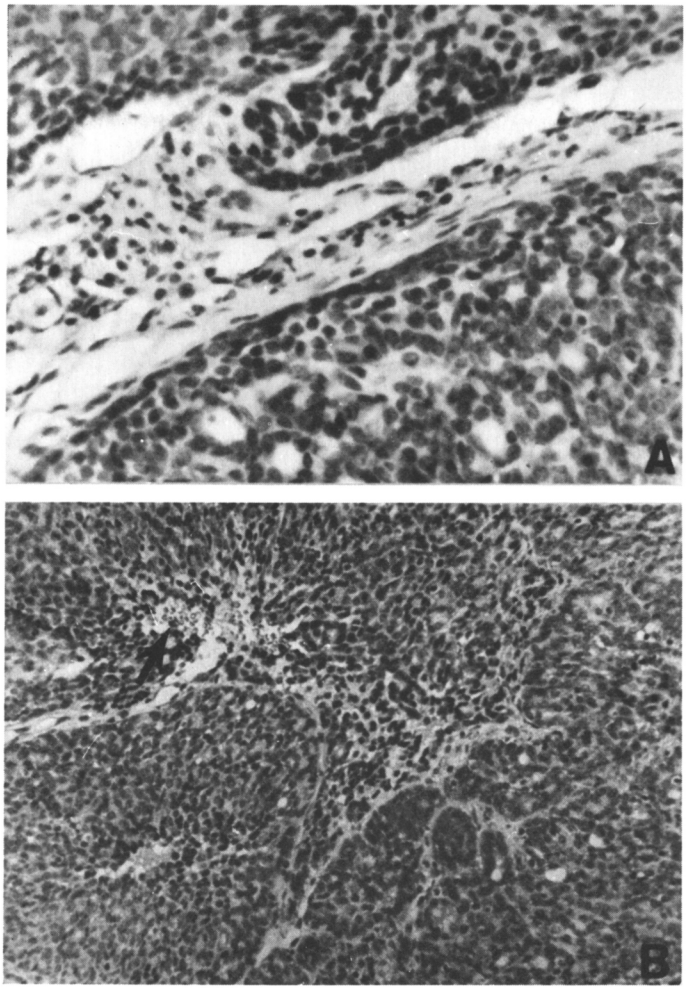

FIG. 4. Mammary tumors at 3 hr postinjection with SFIII. Most tumors (A and B) show inflammatory cell infiltrates and areas of interlobular hemorrhage (arrow) (mag. A, 300×; B, 150×).

edematous tumors, however, remained unchanged. One or more ecchymotic areas were evident in the surface, interspersed with white foci. The appearance of hemisected tumors was characterized by extensive hemorrhage and by gray-white regions. One or two areas oozed a milky exudate. Tissue sections revealed that most of the interalveolar connective tissue had broken down and was replaced by massive areas of hemorrhage within affected lobules; however, many lobules appeared unaffected. Breakdown of the tumor resulted in fragmentation of the tumor mass and the appearance of irregular cavitations containing hemorrhage and/or cellular debris. The tissue in and around the cavitations (Fig. 6) was infiltrated by monocytes, lymphocytes, and plasma cells. The tumor cells at the edges of the cavitations often showed cytoplasmic swelling and vacuolation as well as nuclear hyperchromatism, pyknosis, and fragmentation. The remaining connective tissue appeared hyalinized and showed an infiltration of lymphocytes, monocytes, and plasma cells.

By 48 hr postinjection, the volume of the tumors had decreased by approximately 25–50%. Petechiae and several areas of necrosis were evident on the surface of intact

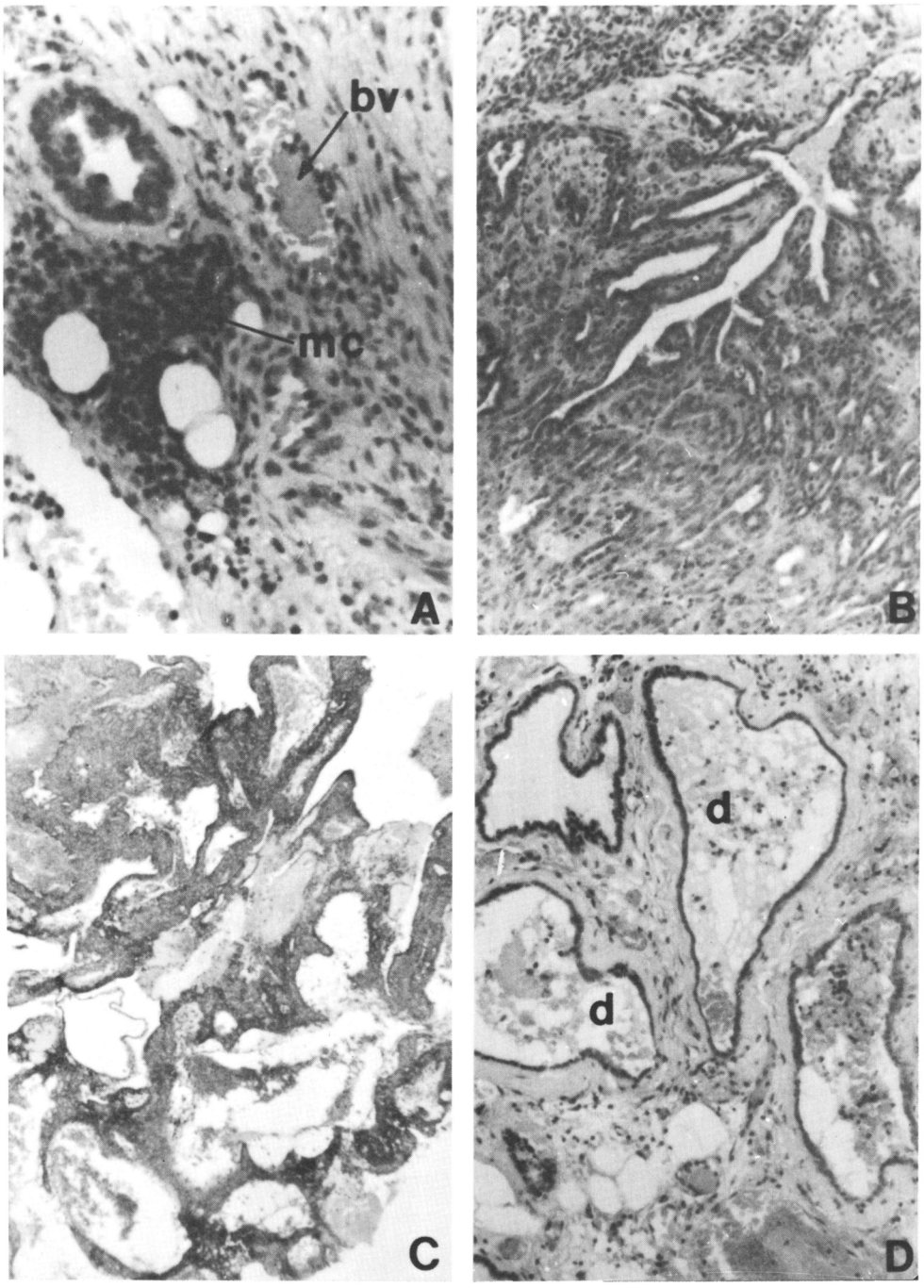

FIG. 5. Mammary tumors of 12 hr post-SFIII-injected mice show mononuclear cell infiltration (mc) and congested blood vessels (bv) in the interlobular connective tissue or the connective tissue has disappeared (B). Pronounced breakdown and cavitations (C) are evident and lactiferous ducts (d) are filled with debris (D). (mag. A, 300×; B, 150×; C, 60×; D, 150×).

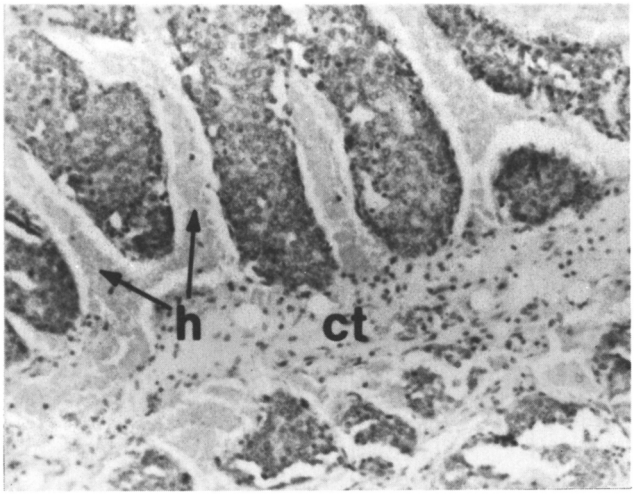

FIG. 6. Mammary tumors at 24 hr postinjection show replacement of the interalveolar connective tissue by cavitations filled with hemorrhage material (h). The hyalinized connective tissue around the cavitations is infiltrated by mononuclear inflammatory cells (ct) (mag. 150×).

and bisected tumors. The characteristics of the tissue sections appeared as a quantitative extension of the 24-hr effects. These included several lobules exhibiting central regions of caseation surrounded by intact tumor tissue; other lobules containing small cavitations, some filled with cellular debris and PMNs; tumor fragmentation; and hemorrhagic foci in both the tumorous lobules and some of the perilobular connective tissue. Other regions of the connective tissue showed large areas of collagenolysis and infiltration by inflammatory cells.

The volume of 72-hr postinjection tumors had decreased by approximately 50%. The exterior and cut surfaces of these boggy neoplasms displayed huge hemorrhagic areas and were spotted with necrotic foci. The architecture and cellular integrity of affected tumorous lobules were completely destroyed and the tissue appeared as an amorphous mass (Fig. 7A). Several massive areas of breakdown resulted in huge cavitations filled with cellular debris, hemorrhage, and caseous material (Fig. 7B). At the edges of these developing irregular cavitations, tumor cells showing nuclear fragmentation and some persistent blood vessels were present. Within the amorphous masses, vascular channels displaying disrupted and discontinuous walls were seen in close proximity to the debris, with extravasated blood adjacent to the mass. The debris contained large numbers of PMNs, lymphocytes, and monocytes, and coagulated tumor cells. The larger lactiferous ducts remained intact and were often filled with red blood cells, nests of tumor cells, and debris similar to the amorphous masses of degenerating tumor. Throughout the tumor, various degrees of breakdown were evident encompassing all the changes seen at 3 through 48 hr postinjection. Other areas showed infiltration of the connective tissue by PMNs, lymphocytes, and monocytes but no apparent tumor breakdown.

Ninety-six hours after injection the tumors had decreased in volume by 75–85%, although their external and internal appearance was similar to tumors of 72-hr postinjection animals. Histologically, the tumors possessed one or more large central cavitations in addition to extensive areas of tumor fragmentation, connective tissue and acinar breakdown, and widespread hemorrhage. However, some areas still appeared relatively unaffected. The edges of the large cavitations now exhibited a smoother border comprised of a stratified layer of tumor cells of variable thickness. Many of these tumor cells were swollen or

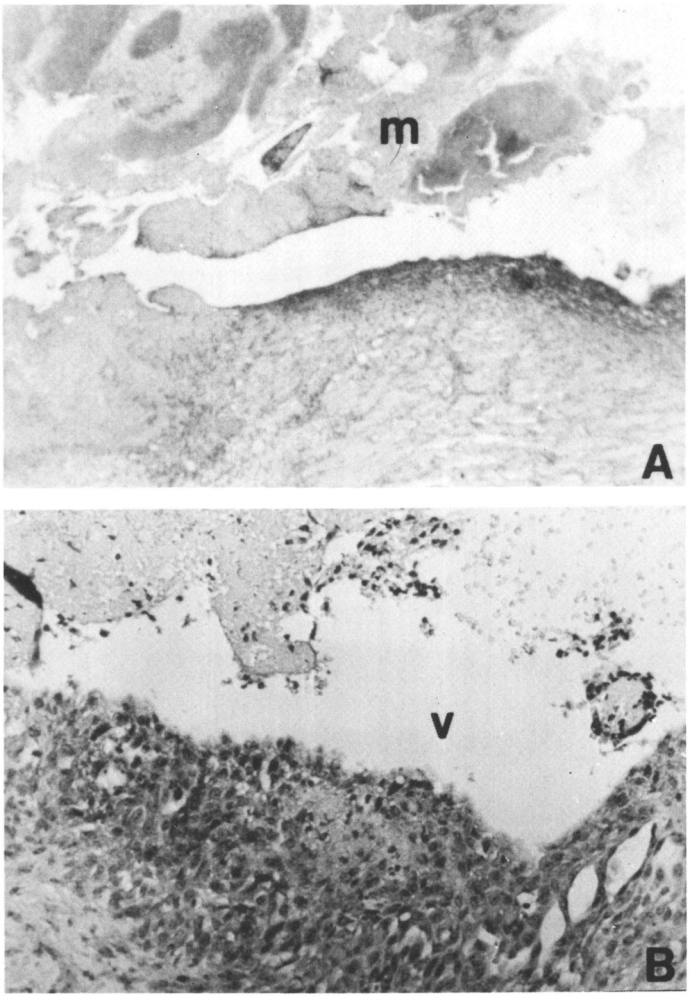

FIG. 7. Mammary tumors of mice at 72 hr postinjection with SFIII show areas where tumor lobules are completely destroyed and replaced by an amorphous mass (m) or huge cavitations (v) (mag. A, 30×; B, 150×).

showed evidence of coagulative necrosis or lysis (Fig. 8A) and were associated with areas of mononuclear cell infiltration (Fig. 8B). Caseous debris was seen within the cavitations. The walls of remaining blood vessels (Fig. 8B) were undergoing breakdown. All regions of the tumor mass showed some degree of change ranging from vascular congestion and slight inflammatory cell infiltrates (Fig. 8C) to complete lysis.

Spontaneous tumor breakdown. Spontaneous tumor breakdown occurred in an animal with a 6-week-old tumor having a volume of approximately 4000 mm^3. The mass was irregular in shape and nodular, with huge areas of soft, edematous, necrotic tissue and hemorrhage. At 30 days after discovery, this tumor displayed progressive, overt breakdown as indicated by changes in its consistency. This spontaneous breakdown has previously been observed only once during the 20 years we have maintained this strain. Hemisection revealed widespread necrosis and hemorrhage, with cheesy material permeating the entire mass. Some small areas of firm, viable tumor tissue still remained. Microscop-

ically, the tumor mass was highly fragmented and showed several large cavitations. In the regions undergoing breakdown (Fig. 9B), the tumor cells exhibited hyperchromatic and pleomorphic nuclei, cytoplasmic swelling, and evidence of cell lysis. The intercellular spaces showed considerable edema. The interlobular connective tissue was either breaking down or absent (Fig. 9C). Regions containing relatively unaffected lobules, which were interspersed with areas of focal necrosis, exhibited inflammatory cell infiltration of the connective tissue (Fig. 9A). Areas of massive destruction contained extravasated blood and amorphous eosinophilic debris. The large cavitations also contained cellular debris.

Nonmammary tissues. Analysis of other organs (liver, lung, kidney, and unaffected mammary glands) of all of the experimental and control animals appeared to be essentially unaffected. Organotypic architecture and cellular structure were unchanged from that of the normal control strain (C3Hf). The lymphoid organs (spleen, lymph nodes, and thymus) did not appear to show any aberrent histological or cytological manifestations. The only notable change which did occur was the appearance of hemosiderin-containing macrophages in the red

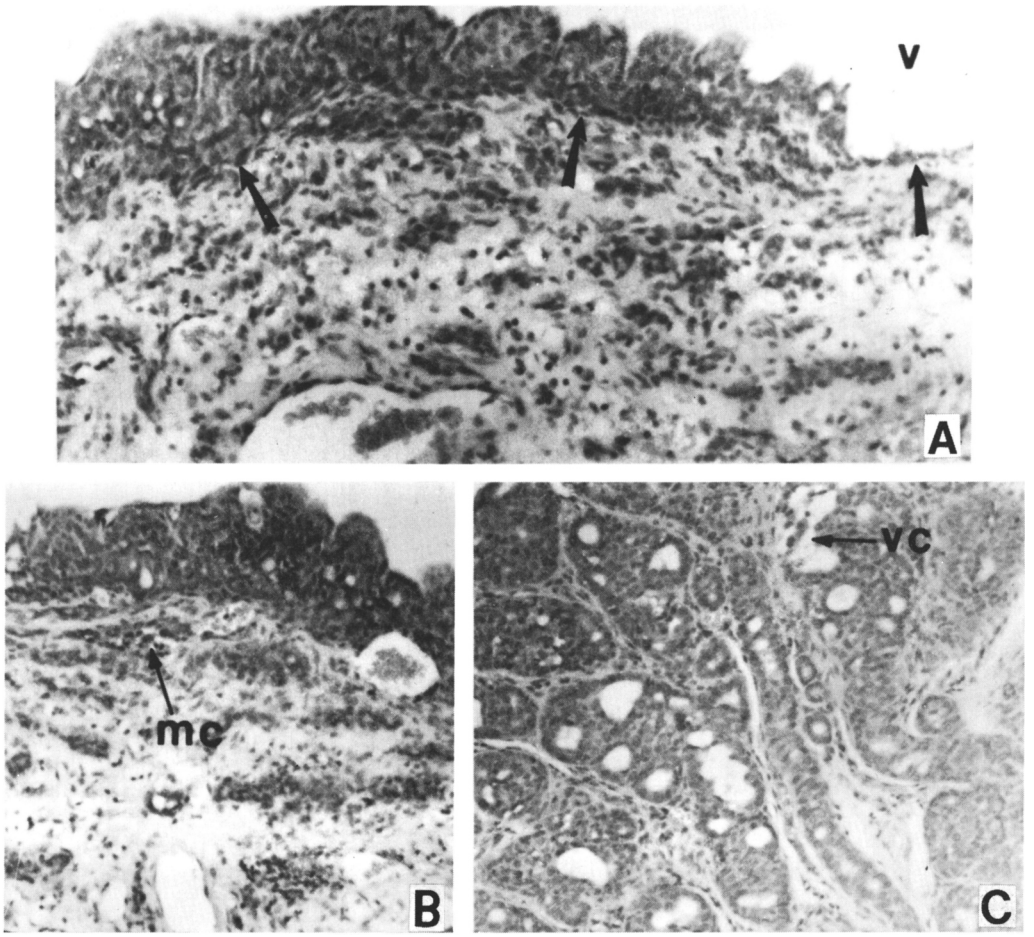

FIG. 8. Mammary tumors 96 hr postinjection with SFIII show large voids (v) bordered by a stratified layer of tumor cells of variable thickness (arrows). These cavitations are associated with areas of mononuclear cell infiltration (mc). Relatively unaffected areas (8C), which are intermixed with regions of necrosis, show vascular congestion (vc) (mag. A, 210×; B, 145×; C, 145×).

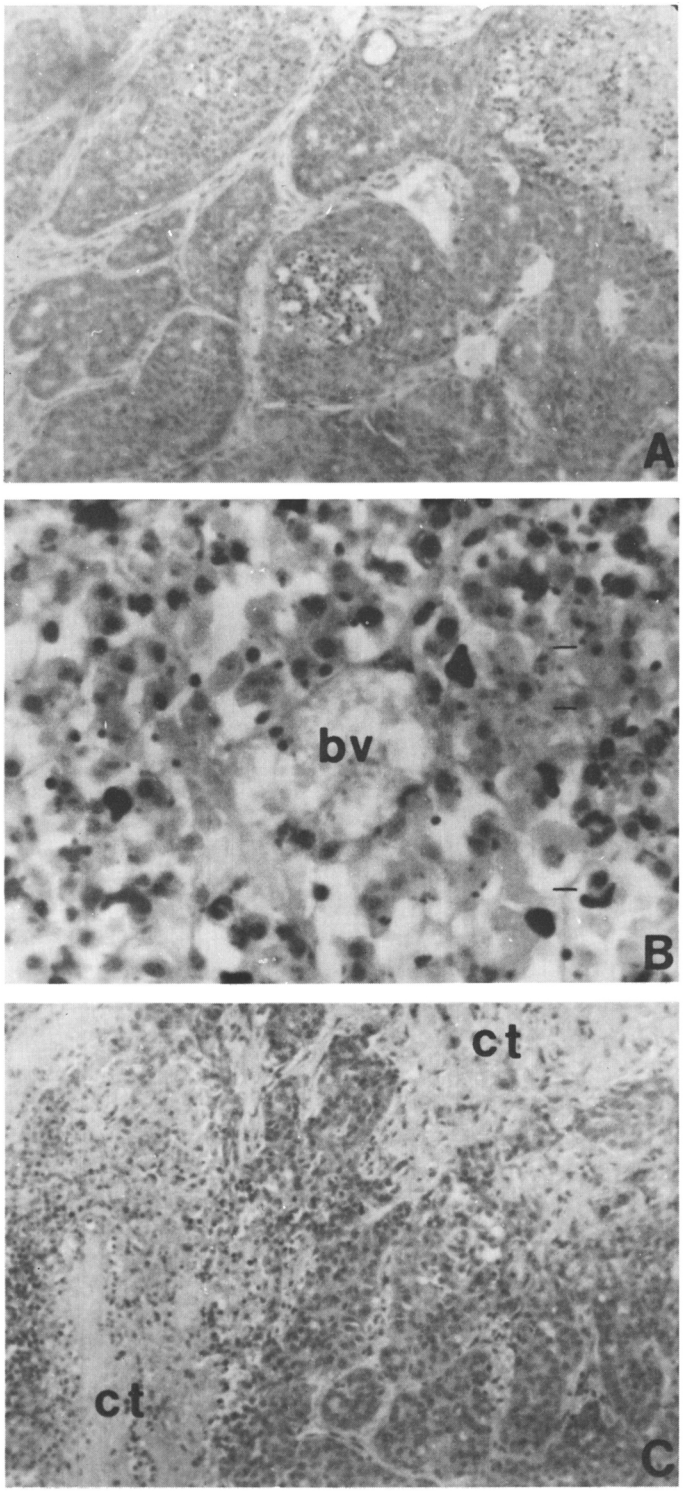

FIG. 9. The mammary tumor of a C3H(T/F) mouse undergoing spontaneous breakdown still shows regions of normal tumor architecture (A). Massive cell lysis is evident in the regions undergoing breakdown (B), though blood vessels (bv) are still present. The interlobular connective tissue (ct) of other areas (C) show evidence of lysis (mag. A, 150×; B, 600×; C, 150×).

pulp of the spleen. These cells appeared at 12 hr postinjection and increased, both in number and size of the cells, throughout the period of observation. Concomitant with this observation was the presence, beginning at 24 hr, of some hemosiderin-containing macrophages in the cellular exudate present in the bronchioles of the lung.

Discussion. Spontaneous destruction of murine mammary tumors has been reported by Strong (13), Squartini (14), and Heston (15). The nature of this tumor destruction has been described at the gross rather than the histopathologic level. Thus, the histopathology of spontaneous tumor destruction reported in the present work affords significant insight into *in vivo* tumor breakdown, as compared to induced tumor lysis.

The results presented indicate that a serum-derived factor from a murine host bearing spontaneous mammary tumor is capable of inducing an accelerated dissolution of the tumor tissue as well as lysis of its cellular constituents. The sequence of events occurring during this destruction could be delineated into specific temporal phases. The initial phase of this autotumorolytic phenomenon is heralded by the appearance of inflammatory cells in the perivascular areas of interlobular connective tissue.

This sequence of histopathological events occurs only when SFIII is extracted from and reinjected into the original donor bearing a spontaneous mammary tumor. If SFIII is extracted from one syngeneic animal and injected into another, no effect is discernible (9). However, if these crude SFIII preparations are semirefined by column chromatography, a particular fraction (molecular weight about 125,000 daltons) is capable of inducing tumor breakdown in syngeneic hosts. This destruction is histopathologically identical to that induced in tumor-bearing host mice injected with their own serum factor (unpublished results).

Occasionally, the entire tumorolytic sequence is accelerated in some lobules so that 12-hr effects are seen at 3 hr postinjection; or 72-hr effects are seen in 24 hr. This would seem to suggest that either host response capability is variable and/or lytic inductive effects of SFIII are variable. One means of investigating this problem would be to purify SFIII and develop a dose–response assay system. However, the continued variability of host response would not be unexpected, since the cellular population of tumors is extremely heterogeneous.

The histopathological patterns of tumor cell degradation described above strongly suggest that several distinct but related mechanisms participate in tumor cell destruction. These involve inflammatory processes, the immune system, and ischemia.

Those lesions which contain foci of ghost-like, anuclear tumor cells present the pattern of cell death brought about by ischemic necrosis, supported by the presence of congested vessels and hemorrhage. Large nodular aggregates of tumor cells also show the effects of ischemia in that necrosis is located centrally within the nodules.

Some tumors contained large numbers of viable and dead PMNs and macrophages in conjunction with congested vessels, extensive inflammatory edema and, frequently, hemorrhage. These characteristic features of an intense, acute inflammatory process explain the finding of numerous foci of liquefactive necrosis in which only granular debris of dead tumor cells remained. Where such liquefaction is extensive and not recent, large cystic spaces, essentially free of cell debris except at the margins, are formed. These spaces have the appearance of large cavitations in the tumor mass.

In other animals, fragmentation of tumor cells has been found to be associated primarily with lymphocytes rather than PMNs and macrophages. This pattern is strongly suggestive of a cell-mediated immune response to tumor antigens. Nevertheless, examination of the spleen, lymph nodes, and thymus of all experimental animals did not appear to show any significant immune reactivity.

Examination of all organs of SFIII-injected, uninjected, and buffer-injected animals revealed that loss of tissue structure and cellular lysis is restricted to the tumor tissue. Thus, induced tissue lysis appears to be specific for tumor tissue.

The tumor which had undergone spontaneous breakdown exhibited regions which resemble the cellular and tissue changes observed in all phases of induced tumorolysis. Therefore, the SFIII-induced phenomenon appears to qualitatively simulate the rare spontaneous breakdown of these mammary carcinomas. Since the histopathological characteristics of spontaneous tumor destruction, which is a 30-day process, and that of induced tumor destruction are virtually identical, it can be inferred that induced tumor destruction represents an accelerated sequencing of the tissue destructive processes occurring in spontaneous breakdown. From the above, it is suggested that spontaneous tumor lysis may be possible at a greater frequency than is observed to occur but that this potential is being thwarted. Previous observations (9) indicated that an inhibitor of this tumor lysis coexists in the blood of the tumor-bearing animal. Nevertheless, the ability to induce tumor breakdown, at will, provides decided advantages in further studies of this mechanism.

Reports of tumor necrotizing factors in murine and nonmurine tumor systems have been related to either endotoxins or to a substance present in sera of nonneoplastic (normal) animals. Most of these studies have emphasized the role of immune mechanisms in this *in vitro* tumor destruction. These include: macrophage arming factors (16, 17); antibody-mediated cytotoxicity (18); T-cell-mediated cytotoxicity (19); macrophage-mediated entity (20, 21); complement in antileukemic action (22); and mononuclear phagocytic involvement (23, 24). Although the presence of lymphocytes in the inflammatory exudate suggests the possibility of an immune response in the process of *in vivo* tumor breakdown, the question of whether these inflammatory cells are specifically attracted to tumor cells or to an area of general inflammation remains unresolved. This enigma has been reviewed in human tumors by Underwood (25).

An alternative explanation of this autoinduced tumor lysis is the action of intracellular tumor cell lysosomes (26). This hypothesis proposes that a localized decline in cellular pH (as a result of increased temperature, localized hypoxia, injury, and/or inflammation) could induce a structural change in biomembranes resulting in the activation of lysosomal enzymes which, in turn, could lead to tumor cell lysis and necrosis. This hypothesis is compatible with the explanation of a tumor outgrowing its blood supply and resulting in cell death. This lowering of pH provides the proper environment for intracellular lysosomal activity. Our examination of tissue samples of young tumors indicates signs of tumor cell death. Yet, these tumors, small in size and early in genesis, are well vascularized. Consequently, the explanation of tumor death as a result of poor vascularization does not seem to be tenable in this situation. Nevertheless, it is possible that injected SFIII could trigger a series of physiochemical changes which would result in localized decreased pH in a short period of time and, therefore, encourage autolytic activity by lysosomal enzymes. This explanation, of course, prompts the query: why does this happen only in tumor cells and not in neighboring normal cells? One means of attempting to answer this query would be to "tag" purified SFIII with a fluorescent or radioactive marker, and follow its specific histological localization with time.

The ability to induce tumor destruction in this tumor model, which apparently simulates the spontaneous destructive phenomenon, affords exceptional opportunities to study the interrelationship of tumor lysis to tumor growth. Sequential histological studies, as carried out in the foregoing study, could provide significant information concerning the source and target tissue of autotumorolytic factors in spontaneous tumor systems. For example, the observation that interlobular tumor connective tissue seems to be the initial target tissue in the lytic process prompts a closer examination of this tissue's properties in tumor and nontumor animals.

The authors wish to thank Mrs. Alba Velez and Mrs. Margaret Andrews for their excellent technical assistance and Miss Shirley Greene for her help in the preparation of this manuscript.

1. Blair P. The mammary tumor virus (MTV). Curr Topics Microbiol Immunol **45**:1–68, 1968.
2. Nandi S, McGrath CM. Mammary neoplasia in mice. Advan Cancer Res **17**:353–414, 1973.
3. Welsch CW, Nagasawa H. Prolactin and murine mammary tumorigenesis. Cancer Res **37**:951–963, 1977.
4. Moore D, Long CA, Vaidya AB, Sheffield JD, Dion AS, Las Fargues EY. Mammary tumor viruses. Advan Cancer Res **29**:347–418, 1979.
5. Dunn TB. Morphology of mammary tumors in mice. In: Homberger F, Fishman M, eds. Physiopathology of Cancer. New York, Hoeber & Harper, p38, 1953.
6. Dux A. Pathology of solid tumors in mice. Int Union Cancer Tech Rep Ser **20**:36–39, 1975.
7. Squartini F. Tumours of the mammary gland. In: Turusov VS, ed. Pathology of Tumors in Laboratory Animals, Tumors of the Mouse. Lyon, International Agency for Research on Cancer, Vol 2: p43, 1979.
8. DeOme KB, Nandi S, Bern HA, Blair P, Pitelka D. The preneoplastic hyperplastic alveolar nodule as the morphological precursor of mammary cancer in mice. In: Severi L, ed. Morphological Precursors of Cancer. Perugia, Division of Cancer Research, p349, 1962.
9. Friedman F. Tumorlytic activity of autochthonous blood fractions upon spontaneous murine mammary carcinomas. J Surg Oncol **12**:53–60, 1979.
10. Staff of the Roscoe B. Jackson Memorial Laboratory. The existence of nonchromosomal influence in the incidence of mammary tumors in mice. Science **78**:465–466, 1933.
11. Bittner JJ. Some possible effects of nursing on the mammary gland tumor incidence in mice. Science **84**:162–163, 1936.
12. Luna LG. Manual of Histologic Staining Methods of the Armed Forces Institute of Pathology, 3rd ed. New York, McGraw–Hill, 1968.
13. Strong LC. Studies of regression of spontaneous adenocarcinoma in mice. Z Krebsforschung **72**:32–36, 1969.
14. Squartini F. Responsiveness and progression of mammary tumors high-cancer-strain mice. J Nat Cancer Inst **28**:911–926, 1962.
15. Heston WE, Vlahakis G, Tsubura Y. Strain DD, a new high mammary tumor strain, and comparison of DD with strain C3H. J Nat Cancer Inst **32**:237–251, 1964.
16. Yamamura Y. Immunological responses to a murine mammary adenocarcinoma II. Monocyte effector activation by humoral factors. Int J Cancer **19**:717–724, 1977.
17. Haskill JS, Key M, Rador LE, Parthenais E, Korn JH, Fett JW, Yamamura Y, Delustro F, Vesley J, Grant G. The importance of antibody and macrophages in spontaneous and drug induced regression of the T1699 mammary adenocarcinoma. J Reticuloendothel Soc **26**:417–425, 1979.
18. Stolfi RL, Fugmann RA, Stolfi LM, Martin DS. Development and inhibition of cytotoxic antibody against spontaneous murine breast cancer. J Immunol **114**:1824–1830, 1975.
19. Berendt MJ, North RJ, Kirste DP. The immunological basis of endotoxin-induced tumor regression. Requirement for T-cell mediated immunity. J Exp Med **148**:1550–1559, 1978.
20. Kurisu M, Dohi N, Yamazaki M, Mizuno D. Macrophage–tumor interaction induced by antibody in antibody-dependent, macrophage-mediated tumor lysis. J Reticuloendothel Soc **28**:237–248, 1980.
21. Old LJ. Cancer immunology: The search for specificity—G.H.A. Clowes Memorial Lecture. Cancer Res **41**:361–375, 1981.
22. Kassel RL, Old LJ, Day NK, Hardy WD. Plasma-mediated leukemia cell destruction: Concentration and purification of the antileukemia factor. Proc Soc Exp Biol Med **155**:230–233, 1977.
23. Matthews N, Watkins FJ. Tumour-necrosis factor from the rabbit. I. Mode of action, specificity and physiochemical properties. Brit J Cancer **38**:302–309, 1978.
24. Matthews N, Ryley HC, Neale L. Tumour-necrosis factor from the rabbit. IV. Purification and chemical characterization. Brit J Cancer **42**:416–422, 1980.
25. Underwood JCE. Lymphoreticular infiltration in humor tumors: Prognostic and biological implications: A review. Brit J Cancer **30**:538–547, 1974.
26. Von Ardenne M, Krüger W. Local tissue hyperacidification and lysosomes. In: Dingle JT, Jacques PJ, Shaw IH, eds. Lysosomes in Applied Biology and Therapeutics. Amsterdam, North-Holland, p161, 1979.

Received September 2, 1981. P.S.E.B.M. 1982, Vol. 169.